

## Dual role of ERK5 in the regulation of T cell receptor expression at the T cell surface

Xavier Rovira-Clavé,\* Maria Angulo-Ibáñez,\* Cathy Tournier,<sup>†</sup> Manuel Reina,\*<sup>1</sup> and Enric Espel<sup>‡,1</sup>

\*Celltec-UB, Department of Cell Biology, and <sup>†</sup>Department of Physiology and Immunology, Faculty of Biology, Universitat de Barcelona, Barcelona, Spain; and <sup>‡</sup>University of Manchester, Faculty of Life Sciences, Manchester, United Kingdom

RECEIVED JANUARY 28, 2015; REVISED JULY 8, 2015; ACCEPTED AUGUST 5, 2015. DOI: 10.1189/jlb.2A0115-034R

### ABSTRACT

Regulation of the levels of the TCR/CD3 complex at the cell surface is critical to proper T cell development and mature T cell activation. We provide evidence that the MAPK ERK5 regulates the surface expression of the TCR/CD3 complex by controlling the degradation of the CD3 $\zeta$  chain and the recovery of the complex after anti-CD3 $\epsilon$  stimulation. ERK5 knockdown led to TCR/CD3 up-regulation at the cell surface and increased amounts of the CD3 $\zeta$  chain. Inhibition of the MEK5-dependent phosphorylation status of the kinase domain of ERK5 in human T CD4<sup>+</sup> cells reduced CD3 $\zeta$  ubiquitination and degradation, limiting TCR/CD3 down-regulation in anti-CD3-stimulated cells. Moreover, TCR/CD3 recovery at the cell surface, after anti-CD3 $\epsilon$  treatment, is impaired by ERK5 knockdown or pharmacological inhibition of autophosphorylation in the ERK5 C-terminal region. ERK5 loss in thymocytes augmented cellular CD3 $\zeta$  and increased cell surface levels of TCR/CD3 on CD4<sup>+</sup>CD8<sup>+</sup> thymocytes. This correlated with enhanced generation of CD4<sup>+</sup>CD8<sup>-</sup>CD25<sup>+</sup> thymocytes. Our findings define ERK5 as a novel kinase that modulates the levels of TCR/CD3 at the cell surface by promoting CD3 $\zeta$  degradation and TCR/CD3 recovery after TCR stimulation. *J. Leukoc. Biol.* 99: 000-000; 2016.

### Introduction

T cell activation depends on the TCR/CD3 complex recognizing specific peptides on the MHC. The TCR/CD3 complex is a multimeric receptor composed of 4 noncovalently attached dimers: the antigen-binding TCR- $\alpha\beta$ , as well as CD3 $\epsilon\gamma$ , CD3 $\epsilon\delta$ , and CD3 $\zeta\zeta$  chains. Regulation of TCR/CD3 complex levels on the cell surface is a dynamic phenomenon that is coordinated through multiple pathways to ensure correct signal transmission.

Abbreviations: AICD = activation-induced cell death, APC = allophycocyanin, DP = double-positive, EGFP = enhanced GFP, Foxp3 = forkhead box p3, Lamp-1 = lysosomal-associated membrane protein 1, LAPTM5 = lysosomal protein transmembrane 5, loxP = locus of crossover of P1, MFI = mean fluorescence intensity, MHC-I = MHC class I, sh = short hairpin, shS = scrambled sh sequence, SLAP = Src-like adaptor protein, SP = single-positive, TEY domain = threonine-glutamic acid-tyrosine activation domain, T<sub>reg</sub> = regulatory T cell, tT<sub>reg</sub> = thymus-derived regulatory T cell

The online version of this paper, found at [www.jleukbio.org](http://www.jleukbio.org), includes supplemental information.

The cell-surface levels of the TCR/CD3 complex present a balance among internalization, recycling, and degradation of existing complexes and the expression of new ones that must be fully assembled before reaching the cell surface [1]. Expression of the TCR/CD3 complex in mature T cells is stable and shows a cycling behavior, with ~30% of the complexes found within endosomal compartments [2]. However, stimulation by TCR/CD3 triggers its rapid down-regulation by enhancing internalization and degradation and reducing recycling [3], thereby avoiding T cell hyperactivation and autoimmunity [4]. In the thymus, thymocytes at the DP stage express 10-fold less TCR/CD3 on the cell surface than SP cells, which is a hypothetical control mechanism for negative and positive selection [5].

ERK5, also known as MAPK7 or big MAPK1, is a member of the MAPK family. The better studied ERK1/2, p38, and JNK kinases play key roles during thymocyte development and in mature T cells after TCR/CD3 stimulation [6]. ERK5 consists of an N-terminal region with a TEY domain, similarly to ERK1/2, and a large C-terminal region with transcriptional activity after autophosphorylation [7]. ERK5 activation occurs by dual phosphorylation of its TEY domain that is mediated by MEK5 [8]. The MEK5/ERK5 pathway is essential for proper blood vessel and cardiac development; thus, ERK5-deficient mice typically die at d 10 or 11 of gestation [9]. In addition, ERK5 is strongly implicated in tumorigenesis, and targeted use as an anti-cancer therapy has been investigated [10, 11]. During T cell development, TCR/CD3 stimulation by strong or weak agonists activates the MEK5-ERK5 pathway and helps to regulate negative selection [12]. It is also known that ERK5 is phosphorylated in peripheral T cells upon TCR/CD3 stimulation [12–15] and that silencing ERK5 in DO11.10 hybridoma cells and primary murine T cells enhances their activation [15]. However, studies that use conditional deletion of *Erk5* in CD4<sup>+</sup> cells show unaltered T cell development and peripheral T cell maintenance [14, 16]. Therefore, the contribution of ERK5 to T cell biology is not fully understood.

In this study, we use genetic and pharmacological approaches in human and mouse T cells to demonstrate that ERK5 promotes CD3 $\zeta$  degradation and TCR/CD3 recovery after anti-CD3 $\epsilon$

1. Correspondence: Faculty of Biology, Universitat de Barcelona, Av. Diagonal 643, 08028 Barcelona, Spain. E-mail: eespel@ub.edu (E.E.); mreina@ub.edu (M.R.)

stimulation. Consequently, we show that ERK5 contributes to the control of TCR/CD3 complex expression on the cell surface.

## MATERIALS AND METHODS

### Antibodies and reagents

The mAb anti-human-CD11a (clone MEM-25), anti-human-CD18 (clone MEM-48), and anti-human-MHC-I (clone W6/32) and Annexin V-FITC conjugated were from ImmunoTools (Friesoythe, Germany). The mAb anti-human-TCR- $\alpha/\beta$  (clone IP26), anti-mouse-CD4-APC (clone RM4-5), anti-mouse-CD8-FITC (clone 53-6.3), anti-mouse-CD3 $\epsilon$ -APC (clone 145-2C11), and anti-mouse-CD25-PE (clone 3C7) were from BioLegend (San Diego, CA, USA). Purified no azide/low endotoxin hamster anti-mouse-CD3 $\epsilon$  (clone 145-2C11) was from BD Biosciences (San Jose, CA, USA). The anti-human-CD3 $\epsilon$  mAb (IgG2a; clone 33-2A3) was from Immunostep (Salamanca, Spain). The anti-TCR $\zeta$  (clone 6B10.2) and anti-ubiquitin (clone P4D1) were from Santa Cruz Biotechnology (Santa Cruz, CA, USA). The polyclonal anti-ERK5 was from Cell Signaling Technology (Danvers, MA, USA). Rabbit anti-Lamp-1-Cy3 and anti- $\beta$ -actin (clone AC-40) were from Sigma-Aldrich (St. Louis, MO, USA). Alexa 488-labeled secondary antibodies were all from Life Technologies (Grand Island, NY, USA). The ERK5 inhibitor BIX02188 was from Selleckchem.com (Houston, TX, USA), and XMD8-92 was from Trocris Bioscience (Bristol, United Kingdom). The cycloheximide was from Sigma-Aldrich.

### Mice

ERK5<sup>loxP/loxP</sup> mice on a C57BL/6 background were described previously in ref. [14]. ERK5<sup>loxP/loxP</sup> mice were bred to Vav-Cre mice (kindly provided by Thomas Graf, Centre for Genomic Regulation, Universitat Pompeu Fabra, Barcelona, Spain) [17] and Foxp3<sup>EGFP</sup> reporter mice (kindly provided by Thomas Stratmann, Universitat de Barcelona, Barcelona, Spain). All mice were treated in accordance with institutional guidelines and national laws and policies. Experiments were conducted on 4-wk-old mice.

### Isolation of murine splenocytes and cell cultures

The spleens were extracted freshly by dissection and disaggregated mechanically to obtain a single-cell suspension. The splenocytes were treated with RBC lysis buffer for 15 min at room temperature before being pelleted by centrifugation and then cultured to  $10^7$  cells/ml. Murine splenocytes, primary human T cells, Jurkat, shS cells, and shERK5 cells were cultured in RPMI, supplemented with 10% FCS, 2 mM L-glutamine, and penicillin/streptomycin and maintained at 37°C in 5% CO<sub>2</sub>.

### Murine DP thymocyte purification

Thymuses were extracted freshly by dissection and disaggregated mechanically to obtain a single-cell suspension. DP thymocytes were purified by sorting on a FACSAria (BD Biosciences), by gating on the CD4<sup>+</sup> and CD8<sup>+</sup> population (purities up to 95% were obtained). The cells were lysed and analyzed by Western blotting or real-time PCR.

### Generation of stable cell lines

Jurkat E6.1 human T cells were obtained from the European Collection of Cell Cultures (Sigma-Aldrich). One million Jurkat T cells were stably transfected by electroporation (Multiporator; Eppendorf, Hamburg, Germany) with a scrambled shRNA expression vector or ERK5-specific shRNA expression vector directed to a conserved *Erk5* sequence in exon 2 (ref. TRCN0000001354; Sigma-Aldrich) and cultured in 10 wells of 24-well plates with medium containing 1  $\mu$ g/ml puromycin. A total of 9 shS and 10 shERK5 cell lines was obtained and used in this study.

### Isolation of human T cells

All of the studies involving human samples were approved by the Ethics Committee of the Universitat de Barcelona. Primary human T cells of healthy

blood donors were obtained from buffy coats at Banc de Sang i Teixits (Blood and Tissue Bank, Barcelona, Spain). PBMCs were isolated by a Ficoll 1.007 density gradient (Lymphoprep, ref. 1114545; Axis-Shield, Dundee, Scotland), and resting T CD4<sup>+</sup> cells were purified by negative selection by use of affinity chromatography (Cedarlane, Ontario, Canada), as described in the manufacturer's protocol (typical purity = 90%). To prepare activated human T CD4<sup>+</sup> cells, resting T CD4<sup>+</sup> cells were activated with PHA (10  $\mu$ g/ml), anti-CD28 (hybridoma CK248 supernatant), and IL-2 (20 U/ml). After 3 d at 37°C, T cells were washed twice and cultured for 1 d in RPMI (ref. BE12-702F; Lonza, Basel, Switzerland) and 10% FCS before their use in experiments.

### Real-time quantitative PCR

Cells were lysed, their total RNA was reverse transcribed (SuperScript III, ref. 11752-050; Life Technologies), and real-time PCR was performed in the StepOne Real-Time PCR system (Applied Biosystems, Life Technologies) by use of GoTaq qPCR Master Mix (ref. A6001; Promega, Madison, WI, USA). The oligonucleotides used for human ERK5 were 5'-GCCTATGGAGTGGTGTCTC-3' (sense) and 5'-GGTCGCTTTCCATCAGGTC-3' (antisense). The oligonucleotides used for human CD3 $\zeta$  were 5'-CAGCCTCTTCTGAGGAAA-3' (sense) and 5'-TCTCAGGAAACAAGGCAGTGA-3' (antisense). The oligonucleotides used for mouse CD3 $\zeta$  were 5'-AGCCCTGTACCTGAGAGCAA-3' (sense) and 5'-CTGTTTGCCCTCCCATCTCTG-3' (antisense). For all samples, the expression levels were normalized to 18S RNA with oligonucleotides from TATAA Biocenter (Göteborg, Sweden; ref. RRN18S). The relative quantification value was calculated as described elsewhere [18].

### Western blot

A total cell extract was prepared from  $10^6$  cells dissolved in 100  $\mu$ l of an SDS loading buffer. The cell extract was incubated at 95°C for 30 min before loading on 8, 10, or 12% SDS polyacrylamide gel and then transferred to a nitrocellulose membrane. Western blots were quantitated by chemiluminescent detection by use of a Kodak X-Omat film or a Luminescent Image Analyzer LAS-3000 (Fujifilm, Tokyo, Japan). Densitometric analysis of proteins was performed by use of Fiji software. All analysis involved normalizing to actin as a loading control.

### Flow cytometry

Flow cytometric analyses were performed as described previously [19]. Samples were analyzed on a Gallios flow cytometer (Beckman Coulter, Brea, CA, USA). Apoptosis was determined by incubating the thymocytes in binding buffer (10 mM Hepes pH 7.4, 140 mM NaCl, 2.5 mM CaCl<sub>2</sub>) with Annexin V-FITC and propidium iodide.

### Confocal microscopy

Cells were fixed, permeabilized, and stained as in intracellular flow cytometry with mouse antibodies against CD3 $\epsilon$  or CD3 $\zeta$  and rabbit antibody against LAMP-1 conjugated with Cy3. Then, cells were washed and incubated with anti-mouse Alexa 488 (Invitrogen). Finally, the cells were washed and resuspended in 7  $\mu$ l Fluoromount mounting medium, applied to microscope slides, and covered with coverslips. Immunostained samples were viewed under a Leica TCS-SPE confocal microscope at Leitz Plan apochromatic 60 $\times$  (NA, 0.7, oil) objective at room temperature. Pictures were acquired by use of the Leica Application Suite software. Final images were processed by Fiji software.

### CD3 $\zeta$ ubiquitination analysis

For the immunoprecipitation experiments,  $50 \times 10^6$  PBMCs were treated with DMSO or BIX02188 (10  $\mu$ M). After 1 h at 37°C, the cells were stimulated with anti-CD3 $\epsilon$  (clone 33-2A3; 0.3  $\mu$ g/ml) for 6 h, washed twice, and lysed in a 1 ml lysis buffer (10 mM Tris HCl, pH 7.5, 10 mM NaCl, 1% Triton X-100, 2.5 mM DTT, 0.1 mM EDTA, 0.1 mM EGTA, and inhibitors of proteases and phosphatases). The lysates were precleared overnight at 4°C with agarose beads, immunoprecipitated with CD3 $\zeta$  antibody, and separated by SDS-PAGE

before Western blotting. The membrane was probed with ubiquitin antibody or CD3 $\zeta$  antibody.

### TUNEL assay

The thymuses were fixed immediately after killing with 10% neutral formalin and embedded in paraffin. Thin tissue sections were cut at 10  $\mu$ m and deparaffinized before TUNEL staining was performed by use of an In Situ Cell Death Detection Kit (ref. 12156792910; Roche Diagnostics, Indianapolis, IN, USA), according to the manufacturer's protocol. The thymus sections were visualized with an Olympus BX61 epifluorescence microscope by use of a  $\times 20$  objective, and images were taken with an Olympus DP70 camera. The final images were processed by Fiji software.

### Statistics

Data are expressed as the means  $\pm$  sd from 3 or more independent experiments. Differences between groups were compared by use of Student *t* tests for 2 groups; 2-way ANOVA with Bonferroni post hoc correction was used for groups with 2 independent variables. Statistical analysis was carried out by use of GraphPad Prism (GraphPad Software, La Jolla, CA, USA). Significance levels are indicated in the figure legends.

## RESULTS

### ERK5 knockdown in Jurkat T cells led to higher cell-surface levels of TCR/CD3

To define the role of ERK5 in T cells, we initially targeted ERK5 in Jurkat leukemic T CD4<sup>+</sup> cells by use of shRNA-mediated knockdown directed to a conserved *Erk5* sequence in exon 2 (shERK5; Fig. 1A and B). Interestingly, ERK5 reduction led to higher levels of CD3 $\epsilon$  (Fig. 1C) and TCR- $\alpha/\beta$  (Fig. 1D) at the cell surface compared with control cell lines transfected with shS. Up-regulation of CD3 $\epsilon$  and TCR- $\alpha/\beta$  by ERK5 knockdown was specific, as the expression of other abundant cell membrane proteins, such as MHC-I (Supplemental Fig. 1A) or LFA-1 (CD11a/CD18; Supplemental Fig. 1B and C), was not altered. Moreover, CD3 $\epsilon$  up-regulation was not a result of augmented total amounts of this protein in shERK5 cell lines (Fig. 1E). Importantly, TCR/CD3 up-regulation in shERK5 cell lines correlates with an enhanced AICD (Supplemental Fig. 1D). These results suggest a possible role for ERK5 in the regulation of TCR/CD3 expression at the cell surface in Jurkat T cells.

### ERK5 knockdown in Jurkat T cells led to higher CD3 $\zeta$ protein levels and reduced TCR/CD3 recovery at the cell surface after anti-CD3 $\epsilon$ stimulation

Given that the control of CD3 $\zeta$  levels is a key regulatory mechanism for TCR/CD3 complex expression at the cell surface [20], we analyzed the total amount of CD3 $\zeta$  in shERK5 cell lines and observed a significant increase in the expression of CD3 $\zeta$  compared with shS cell lines (Fig. 2A). In contrast, CD3 $\zeta$  mRNA levels were similar in shERK5 and shS cell lines (Fig. 2B), suggesting that CD3 $\zeta$  chain degradation was reduced in shERK5 cell lines. To test this hypothesis, we measured CD3 $\zeta$  half-life by incubating the cells with cycloheximide, an inhibitor of protein synthesis, for up to 6 h (Fig. 2C). CD3 $\zeta$  showed a trend toward an increased half-life in shERK5 cells at 3 h ( $P = 0.061$ ). This difference could account for the incremented CD3 $\zeta$  levels observed in long-term cultured cells. These results show that

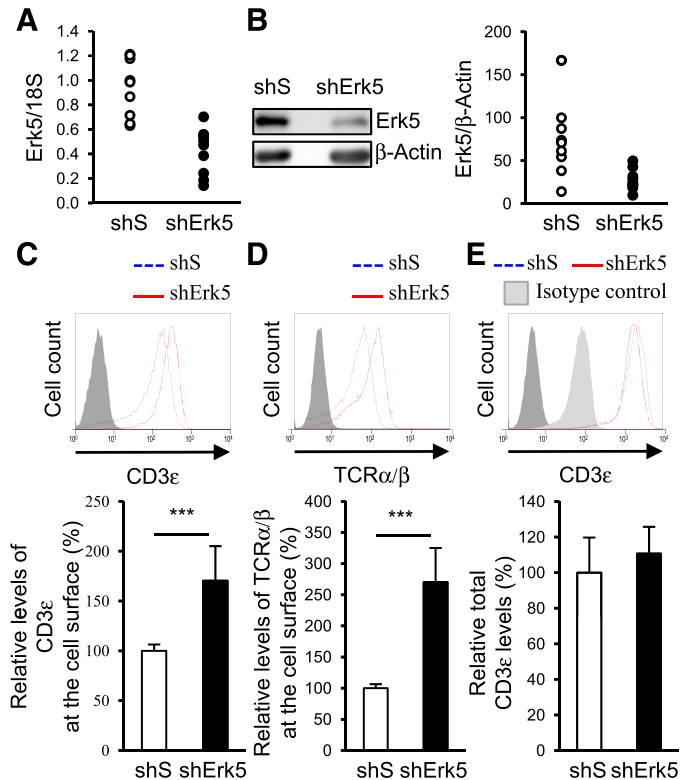


**Figure 1. ERK5 knockdown in Jurkat T cells increased cell-surface levels of TCR/CD3.** (A) ERK5 mRNA levels in shERK5 Jurkat cell lines. ERK5:18S values are normalized to 1 shS cell line, given an arbitrary value of 1.0. (B) ERK5 protein levels in shERK5 Jurkat cell lines. Representative Western blot with anti-ERK5 (left); ERK5: $\beta$ -actin ratio (right). (C and D) Cell-surface expression of CD3 $\epsilon$  (C) and TCR- $\alpha/\beta$  (D). Cells were incubated with anti-CD3 $\epsilon$  or anti-TCR- $\alpha/\beta$ , followed by staining with Alexa 488-conjugated F(ab')<sub>2</sub> anti-mouse antibody and analysis by flow cytometry. Representative histograms (upper); quantification of FACS staining (lower). The MFI is represented as a percentage of the value obtained with the shS cell line. (E) Expression of total CD3 $\epsilon$  (extracellular and intracellular). Representative histogram (upper); quantification of FACS staining (lower). (A and B) Nine and 10 different cell lines were analyzed for shS and shERK5 cell lines, respectively. (C–E) The analyses were repeated with 2 different shS cell lines and 2 different shERK5 cell lines, and the average  $\pm$  sd of 3 independent experiments is presented. \*\*\* $P < 0.001$ .

increased CD3 $\zeta$  expression led to increased TCR/CD3 at the surface of shERK5 Jurkat T cells and suggest a role for ERK5 in the regulation of CD3 $\zeta$  protein levels.

Antigen-stimulated T cells are known to down-regulate TCR/CD3 from the cell surface, a process that rapidly desensitizes the cell [4, 21]. To gain insight in the ERK5 function in the regulation of TCR/CD3 at the cell surface, we promoted TCR/CD3 down-regulation in shS and shERK5 cell lines by stimulation with soluble anti-CD3 $\epsilon$  antibody. Analysis of TCR/CD3 down-regulation by quantitation of cell-surface CD3 $\epsilon$  expression at different time points, showed a similar down-regulation pattern for both shERK5 and control shS cells (Fig. 2D).

The down-regulation of TCR/CD3 in stimulated T cells is reversed after removal of the stimulus [1]. To establish whether

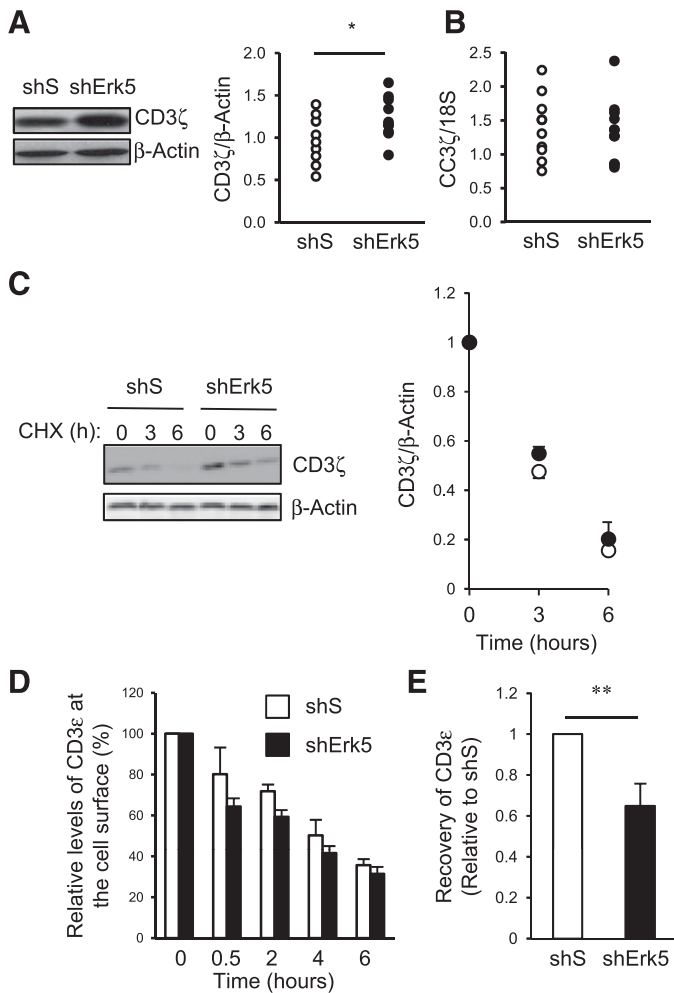


**Figure 2. ERK5 knockdown in Jurkat T cells led to reduced CD3ζ degradation and reduced TCR/CD3 recovery on the cell surface after anti-CD3ε stimulation.** (A) CD3ζ protein levels in shERK5 Jurkat cell lines. Representative Western blot with anti-CD3ζ (left) and CD3ζ:β-actin ratio in 9 different cell lines (right) is presented. (B) CD3ζ mRNA levels in shERK5 cell lines. CD3ζ:18S values in 10 different cell lines were normalized to 1 shS cell line given an arbitrary value of 1.0. (C) CD3ζ protein levels in shERK5 Jurkat cell lines. shS and shERK5 cells were cultured in the presence of cycloheximide (CHX; 25 μg/ml) for different time points. Representative Western blot with anti-CD3ζ (left) and CD3ζ:β-actin ratio (right) are presented. (D) Kinetics of CD3ε down-regulation in shERK5 Jurkat cell lines. shS and shERK5 cells were stimulated with anti-CD3ε (0.3 μg/ml) for different time points at 37°C. The cells were then incubated with saturating amounts of the same anti-CD3ε, followed by staining with Alexa 488-conjugated F(ab')<sub>2</sub> anti-mouse antibody and analyzed by flow cytometry. The MFI is represented as a percentage of the value obtained at time 0. (E) TCR/CD3 recovery after anti-CD3ε treatment in shERK5 Jurkat cell lines. shS and shERK5 cells were treated during 6 h as in D and then washed twice to remove the antibody before culturing them in normal medium during 18 h. Then, the cells were stained as in D. TCR/CD3 recovery was normalized to the shS cell line given an arbitrary value of 1.0. (C–E) The analyses were repeated with 1 shS cell line and 1 shERK5 cell line, and the average ± sd of 3 independent experiments is presented. \**P* < 0.05; \*\**P* < 0.01.

ERK5 controlled the recovery of TCR/CD3 at the cell surface, we treated shERK5 cells with anti-CD3ε over 6 h, washed the cells to remove the antibody, and cultured them in normal medium for

18 h. Unexpectedly, the surface CD3ε levels in shERK5 cells showed a 40% reduction compared with shS cells (Fig. 2E), suggesting that ERK5 may play a positive role in the TCR/CD3 recovery at the cell surface after anti-CD3ε treatment. Taken together, these data support that ERK5 could alter cell-surface expression of TCR/CD3 by acting in 2 different pathways: CD3ζ degradation and TCR/CD3 recovery at cell surface after anti-CD3ε treatment.

### Pharmacological inhibition of ERK5 impaired TCR/CD3 down-regulation and reduced its recovery in anti-CD3ε-stimulated T CD4<sup>+</sup> cells

We next evaluated whether pharmacological inhibition of the MEK5/ERK5 signaling pathway affects TCR/CD3 recovery after anti-CD3ε treatment. The inhibitor BIX02188 suppresses MEK5 catalytic activity and ERK5 phosphorylation in the kinase domain, whereas the inhibitor XMD8-92 blocks ERK5 autophosphorylation at the C-terminal region (Fig. 3A) [7]. At the concentrations used in this study, neither one is known to affect other related MAPKs [10, 11]. Whereas inhibition of the MEK5-dependent phosphorylation status of the ERK5 kinase domain by BIX02188 in TCR<sup>+</sup> PBMCs from healthy donors during TCR/CD3 recovery did not show differences compared with control cells, ERK5 inhibition with XMD8-92 resulted in an impaired capacity to recover normal levels of TCR/CD3 at the cell surface (Fig. 3B). These data suggest that ERK5 regulates TCR/CD3 recovery at the cell surface after anti-CD3ε treatment through autophosphorylation of its C-terminal region and independently of the MEK5-dependent phosphorylation status of its kinase domain.

We also used these pharmacological inhibitors to analyze the effect of ERK5 during TCR/CD3 down-regulation. Interestingly, when Jurkat cells were CD3 stimulated in the presence of BIX02188 or XMD8-92, the down-regulation of TCR/CD3 was impaired (Fig. 3C and Supplemental Fig. 2A and B), suggesting a role for ERK5 in the control of TCR/CD3 down-regulation. To confirm our results in primary human T CD4<sup>+</sup> cells, these were stimulated with soluble anti-CD3ε to induce TCR/CD3 down-regulation in the presence or absence of BIX02188 and XMD8-92. Stimulation of resting (Fig. 3D) or activated (Fig. 3E) T CD4<sup>+</sup> cells with different concentrations of anti-CD3ε led to TCR/CD3 down-regulation, but interestingly, this was significantly impaired in cells treated with BIX02188. This confirmed a role for the MEK5/ERK5 signaling pathway in the regulation of cell-surface levels of TCR/CD3. Treatment with XMD8-92 did not modify TCR/CD3 down-regulation in resting (Fig. 3D) or activated (Fig. 3E) cells, suggesting that autophosphorylation of the C-terminal region of ERK5 was not involved in the regulation of TCR/CD3 down-regulation during anti-CD3ε treatment. The inhibition of the MEK5/ERK5 signaling pathway by BIX02188 did not affect TCR/CD3 down-regulation in the 1st 30 min, but after this time, down-regulation was arrested in BIX02188-treated resting (Fig. 3F) or activated (Fig. 3G) T CD4<sup>+</sup> cells. Of note, stimulation of Jurkat cells with anti-CD3ε led to TCR/CD3 down-regulation of >50% (Fig. 3C and Supplemental Fig. 2A and B), an extent that we did not observe in primary human T CD4<sup>+</sup> cells. This suggested a role for the phosphorylation of the C-terminal domain of ERK5 in the control of TCR/CD3 down-regulation during strong signaling.

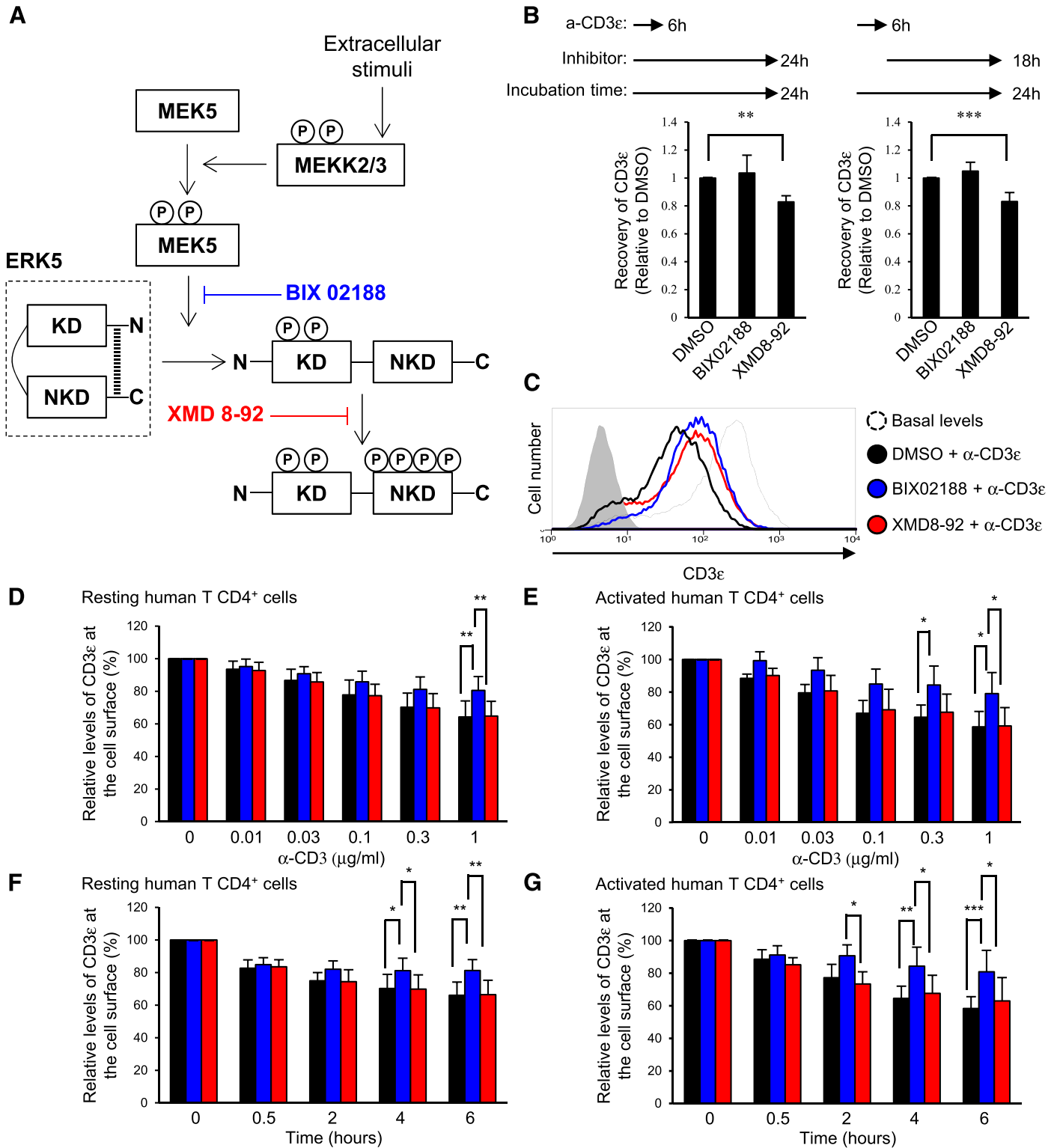


**Figure 3. TCR/CD3 down-regulation by anti-CD3ε treatment is impaired by pharmacological inhibition of ERK5.** (A) Mechanism of action of ERK5 pathway inhibitors. P, phosphorylation; MEKK, MEK kinase; KD, kinase domain; NKD, nonkinase domain; N, N terminus; C, C terminus. (B) TCR/CD3 recovery after anti-CD3ε treatment in TCR<sup>+</sup> PBMCs, which were stimulated with anti-CD3ε (0.3 μg/ml) for 6 h at 37°C in the presence (left) or absence (right) of DMSO, BIX02188 (10 μM), or XMD8-92 (10 μM). Then, cells were washed twice to remove the antibody before culturing them during 18 h in medium with inhibitors and stained as in Fig. 2D. TCR/CD3 recovery was normalized to the shS cell line, given an arbitrary value of 1.0; n = 3. (C) Jurkat T cells treated with DMSO, BIX02188 (10 μM), or XMD8-92 (10 μM). After 1 h at 37°C, cells were stimulated with anti-CD3ε (clone 33-2A3; 0.3 μg/ml) for 4 h at 37°C. The cells were then incubated with saturating amounts of the same anti-CD3ε, followed by staining with Alexa 488-conjugated F(ab')<sub>2</sub> (continued on next page)

**ERK5 controlled CD3ζ ubiquitination and degradation during TCR/CD3 down-regulation**

Results from shERK5 cell lines suggested a role for ERK5 in CD3ζ degradation. To prove it, we treated activated T CD4<sup>+</sup> cells with soluble anti-CD3ε over 6 h to induce CD3ζ degradation in the presence or absence of BIX02188. Whereas cellular levels of CD3ζ decreased with CD3 stimulation, treatment with BIX02188 blocked CD3ζ degradation (Fig. 4A). Importantly, in unstimulated cells, the inhibitor alone does not affect the CD3ζ steady state (Supplemental Fig. 2C), indicating that the kinase domain of ERK5 promotes CD3ζ degradation after CD3 stimulation. Confocal microscopy was then performed to visualize the effect of BIX02188 on CD3ε and CD3ζ distribution in T CD4<sup>+</sup> cells. As expected from flow cytometry and Western blot analysis, CD3 stimulation caused internalization of CD3ε and CD3ζ and reduction of CD3ζ (Fig. 4B), with both phenomena spared by BIX02188 treatment.

After TCR triggering, CD3ζ is known to be targeted by ubiquitination before its degradation [22], so next, we tested whether the pattern of CD3ζ ubiquitination was altered by ERK5 activity. PBMCs were stimulated with soluble anti-CD3ε to induce CD3ζ degradation, in the presence or absence of BIX02188, before cell lysates were prepared, and CD3ζ was immunoprecipitated. As previously seen for T CD4<sup>+</sup> cells (Fig. 4A), treatment of PBMCs with BIX02188 impaired the degradation of CD3ζ produced by CD3 stimulation (whole-cell lysate; Fig. 4C and Supplemental Fig. 2D). However, CD3ζ was less ubiquitinated in cells treated with BIX02188 (Fig. 4C and Supplemental Fig. 2D), suggesting that the kinase domain of ERK5 promoted CD3ζ ubiquitination. Taken together, these results indicate that the kinase domain of ERK5 promoted TCR/CD3 down-regulation by promoting ubiquitination and posterior degradation of CD3ζ.

**Splenic T cells from Erk5<sup>-/-</sup> mice did not show attenuated TCR/CD3 down-regulation**

To obtain insight into the physiologic significance of ERK5 in T cell function, we bred ERK5-floxed mice to Vav-Cre mice to generate ERK5-specific deficiency in the hematopoietic system (called ERK5<sup>-/-</sup>; Supplemental Fig. 3A–C). Neither the T cell cellularity (Supplemental Fig. 3D–E) nor the percentages of T CD4<sup>+</sup> and CD8<sup>+</sup> cells (Supplemental Fig. 3F and G) in the thymus and spleen were altered by the absence of ERK5, which was consistent with previous reports [14, 16] and confirmed that ERK5 was not needed for T cell development and peripheral T cell maintenance.

Our results suggest a role for ERK5 in the regulation of CD3ζ stability and TCR/CD3 traffic; however, steady-state, splenic T cells from ERK5<sup>-/-</sup> and ERK5<sup>+/+</sup> mice had similar amounts of CD3ε at the cell surface (Fig. 5A). Moreover, stimulation of splenocytes with anti-CD3ε at different time points revealed that TCR/CD3 down-regulation was not diminished in the ERK5<sup>-/-</sup> mice

anti-mouse antibody and analyzed by flow cytometry. Representative histogram of cell-surface staining is shown. (D and E) Dose-response and (F and G) kinetics of CD3ε down-regulation. Resting (D and F) and activated (E and G) primary human T CD4<sup>+</sup> cells treated with DMSO, BIX02188 (10 μM), or XMD8-92 (10 μM) for 1 h at 37°C. Then, cells were treated with different anti-CD3ε concentrations or incubation times and stained as in Fig. 2D. The MFI is represented as a percentage of the value obtained at time 0; n = 4. \*P < 0.05; \*\*P < 0.01; \*\*\*P < 0.001.

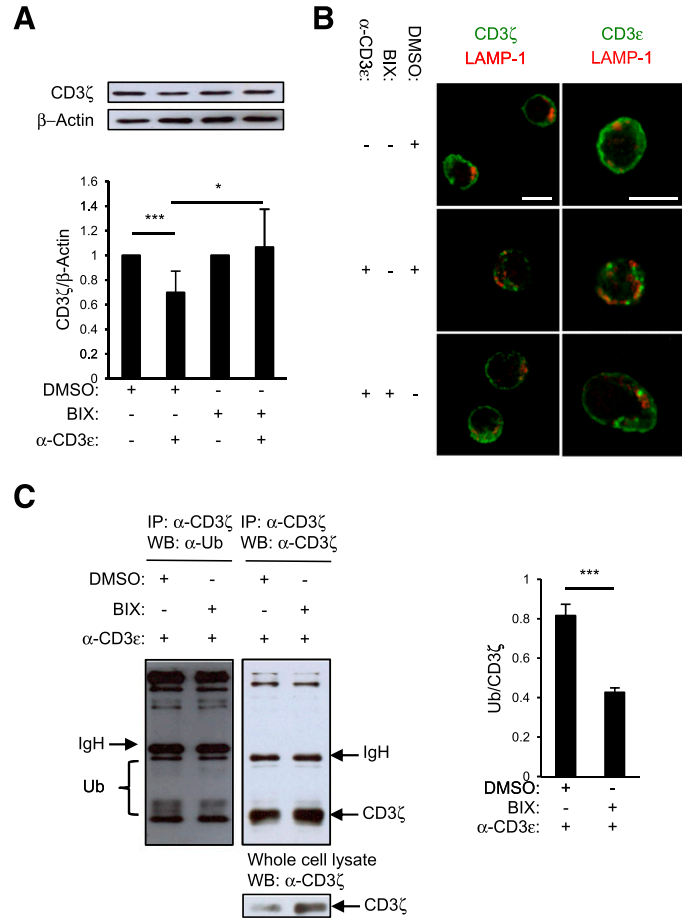


**Figure 4. Inhibition of ERK5 in anti-CD3ε-stimulated primary human T cells impairs CD3ζ ubiquitination and degradation.** (A) CD3ζ degradation after anti-CD3ε treatment. Activated T CD4<sup>+</sup> cells were treated as in Fig. 3F for 6 h. The cell lysates were immunoblotted with anti-CD3ζ. Representative Western blot (upper) and the CD3ζ:β-actin ratio (lower) are presented; n = 7. (B) Intracellular location of CD3ζ (left) and CD3ε (right). Activated human T CD4<sup>+</sup> cells were treated as in A, permeabilized, and stained with antibodies against CD3ζ (green) or CD3ε (green) and LAMP-1 (red). The samples were visualized by confocal microscopy, and representative images are presented. Original scale bars, 10 μm; n = 2. (C) CD3ζ ubiquitination (Ub). PBMCs were treated as in A, and CD3ζ was immunoprecipitated (IP) from PBMCs. Representative immunoblots [left; Western blot (WB)] and ubiquitination:CD3ζ ratio (right) are presented; n = 3. BIX, BIX02188. \*P < 0.05; \*\*\*P < 0.001.

compared with ERK5<sup>+/+</sup> mice (Fig. 5B), suggesting that ERK5 does not control TCR/CD3 down-regulation in murine splenocytes.

**ERK5<sup>-/-</sup> mice showed reduced degradation of CD3ζ in DP thymocytes**

Immature CD4<sup>+</sup>CD8<sup>+</sup> DP thymocytes in the thymus express 10-fold less TCR/CD3 at the cell surface than mature CD4<sup>+</sup> or CD8<sup>+</sup> SP thymocytes because of a constitutive ubiquitination of CD3ζ

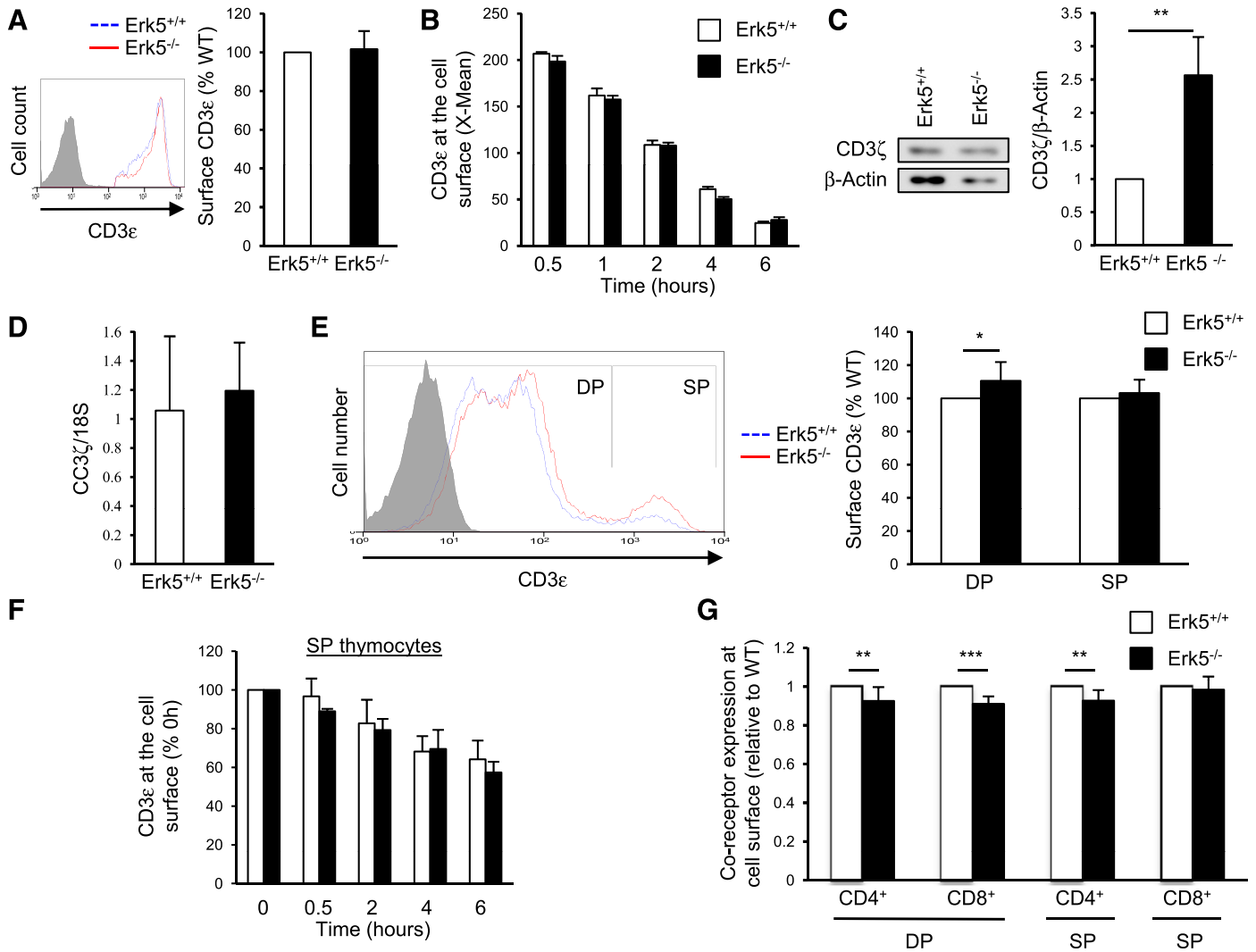


**Figure 5. ERK5<sup>-/-</sup> mice show reduced degradation of CD3ζ in DP thymocytes.** (A) Cell-surface expression of CD3ε on mice splenocytes. Cells were incubated with anti-CD3ε (clone 145-2C11), followed by staining with Alexa 488-conjugated F(ab')<sub>2</sub> anti-hamster antibody and analyzed by flow cytometry. A representative histogram (left) and the MFI (right; as the percentage of the value obtained in ERK5<sup>+/+</sup> mice) are presented. The average ± SD of ERK5<sup>+/+</sup> and ERK5<sup>-/-</sup> mice ( $n = 6$ ) is presented. (B) Kinetics of CD3ε down-regulation. Splenocytes were stimulated with anti-CD3ε (clone 145-2C11; 1 μg/ml) at 37°C for the times indicated. The cells were then incubated with saturating amounts of the same anti-CD3ε and stained with Alexa 488-conjugated F(ab')<sub>2</sub> anti-hamster antibody before analysis by flow cytometry. The average ± SD of ERK5<sup>+/+</sup> ( $n = 3$ ) and ERK5<sup>-/-</sup> ( $n = 4$ ) mice is presented. (C) CD3ζ protein levels in DP thymocytes, which were sorted as described in Materials and Methods. The cell lysates were immunoblotted with anti-CD3ζ. Representative Western blot (left) and the CD3ζ:β-actin ratio (right) are presented. Average ± SD of 3 pairs of ERK5<sup>+/+</sup> and ERK5<sup>-/-</sup> mice is shown. (D) CD3ζ mRNA levels in DP thymocytes. CD3ζ:18S was normalized to ERK5<sup>+/+</sup> mice and given an arbitrary value of 1.0. Average ± SD of 5 pairs of ERK5<sup>+/+</sup> and ERK5<sup>-/-</sup> mice is shown. (E) Cell-surface expression of CD3ε on mice thymocytes. Cells were incubated and stained as in A. Representative histograms showing 2 different cell populations based on CD3ε expression (left). The MFI is represented as a percentage of the value obtained in the DP or SP population in ERK5<sup>+/+</sup> mice (right). Average ± SD of 8 pairs of ERK5<sup>+/+</sup> and ERK5<sup>-/-</sup> mice is shown. (F) Kinetics of CD3ε down-regulation. Thymocytes were stimulated with anti-CD3ε (clone 145-2C11; 1 μg/ml) at 37°C for the times indicated. The cells were then incubated with saturating amounts of the same anti-CD3ε and stained with Alexa 488-conjugated F(ab')<sub>2</sub> anti-hamster antibody before analysis by flow cytometry by gating in the CD3<sup>high</sup> thymocytes. The average ± SD of ERK5<sup>+/+</sup> ( $n = 3$ ) and ERK5<sup>-/-</sup> ( $n = 4$ ) mice is presented. (G) Cell-surface expression of CD4 and CD8 on mice thymocytes, which were stained with anti-CD4-APC and anti-CD8-FITC and analyzed by flow cytometry. The MFI is represented for each marker as a percentage of the value obtained in the DP or SP population in ERK5<sup>+/+</sup> mice. Average ± SD of 9 pairs of ERK5<sup>+/+</sup> and ERK5<sup>-/-</sup> mice is shown. WT, Wild-type. \* $P < 0.05$ ; \*\* $P < 0.01$ ; \*\*\* $P < 0.001$ .

[22]. Given that ERK5 promotes CD3ζ ubiquitination on peripheral T CD4<sup>+</sup> cells after anti-CD3ε stimulation (Fig. 4C), we surmised that ERK5 could play a role in controlling CD3ζ steady state in DP thymocytes. Therefore, we analyzed the total amount of CD3ζ on the immature DP thymocytes of ERK5<sup>-/-</sup> mice and

detected a 2.5-fold increase compared with ERK5<sup>+/+</sup> mice (Fig. 5C). Interestingly, CD3ζ mRNA levels were similar in the DP thymocytes of ERK5<sup>-/-</sup> and ERK5<sup>+/+</sup> mice (Fig. 5D), suggesting that ERK5 promoted CD3ζ degradation. In addition, as CD3ζ degradation regulates TCR/CD3 expression on DP thymocytes

[22], we analyzed CD3 $\epsilon$  expression at the cell surface by flow cytometry. As DP thymocytes express 10-fold less TCR/CD3 at the cell surface than SP cells [5], we separated DP and SP thymocytes by CD3 $\epsilon$  staining intensity (Fig. 5E, histogram). As expected from the analysis of TCR/CD3 expression in splenic T cells (Fig. 5A and B), SP thymocytes from ERK5 $^{-/-}$  and ERK5 $^{+/+}$  mice showed the same levels of cell-surface CD3 $\epsilon$  (Fig. 5E) and the same TCR/CD3 down-regulation profile after anti-CD3 $\epsilon$  treatment (Fig. 5F). However, in DP thymocytes of ERK5 $^{-/-}$  mice, CD3 $\epsilon$  expression on the cell membrane was slightly increased (Fig. 5E), consistent with the increased CD3 $\zeta$  levels in these cells. Thus, ERK5 controlled TCR/CD3 levels at the cell surface of immature DP thymocytes by promoting CD3 $\zeta$  degradation.

Interestingly, cell-surface CD4 and CD8 levels of DP thymocytes and CD4 levels of CD4 $^{+}$  SP thymocytes were slightly down-regulated in ERK5 $^{-/-}$  mice (Fig. 5G). We do not know at this point whether the decrease of CD4 and CD8 in DP thymocytes was an indirect consequence of higher TCR expression or a direct effect of the absence of ERK5. However, changes in the relative abundance of TCR/CD3 receptors or CD4 and CD8 coreceptors could affect the selection process through minimum and maximum signaling thresholds that determine the fate of DP thymocytes, which in turn, could lead to death by neglect and negative selection with weak and strong signals, respectively [5]. ERK5 deficiency in Jurkat T cells promotes AICD after anti-CD3 $\epsilon$  stimulation (Supplemental Fig. 1D), and it has been proposed that the MEK5/ERK5 pathway plays a role in negative selection [12]. However, TUNEL staining to determine if ERK5 influences thymocyte apoptosis showed a similar number of TUNEL $^{+}$  apoptotic thymocytes in ERK5 $^{-/-}$  and ERK5 $^{+/+}$  mice (Fig. 6A and Supplemental Fig. 4A). Moreover, FACS quantification by Annexin V and propidium iodide staining showed the same amount of apoptotic thymocytes in ERK5 $^{-/-}$  compared with ERK5 $^{+/+}$  mice (Fig. 6B). These results indicate that the higher amount of TCR/CD3 at the cell surface of DP thymocytes from ERK5 $^{-/-}$  mice does not promote apoptosis. However, the existence of a potential compensatory phenomenon cannot be excluded at this point.

### ERK5 $^{-/-}$ mice showed an increased percentage of CD4 $^{+}$ CD8 $^{-}$ CD25 $^{+}$ thymocytes and reduced percentage of T $_{reg}$ in the spleen

Up-regulated TCR/CD3 on the cell surface is known to influence the strength of the TCR/CD3 signal by altering TCR avidity for peptide and MHC [1]. During development, CD4 $^{+}$ CD8 $^{-}$ CD25 $^{+}$ Foxp3 $^{+}$  tT $_{reg}$ s experience stronger TCR/CD3 signals than conventional T cells, and a population enriched in tT $_{reg}$  progenitors (CD4 $^{+}$ CD8 $^{-}$ CD25 $^{+}$ Foxp3 $^{-}$ ) receives even stronger TCR/CD3 signals [23]; therefore, we hypothesized that up-regulation of TCR/CD3 at the cell surface of DP thymocytes could increase the presence of CD4 $^{+}$ CD8 $^{-}$ CD25 $^{+}$  thymocytes in ERK5 $^{-/-}$  mice. To examine the effect of ERK5 deficiency in the development of this thymocyte subpopulation, we analyzed the percentage of CD4 $^{+}$ CD8 $^{-}$ CD25 $^{+}$  cells in the thymus by flow cytometry. Compared with ERK5 $^{+/+}$  mice, the absence of ERK5 increased the CD4 $^{+}$ CD8 $^{-}$ CD25 $^{+}$  population in the thymus (Fig. 6C), suggesting that ERK5 limited the generation of CD4 $^{+}$ CD8 $^{-}$ CD25 $^{+}$  thymocytes by down-regulating TCR/CD3 at the cell surface of

DP thymocytes via degradation of CD3 $\zeta$ . To examine further the effect of ERK5 on T $_{reg}$  development, we bred Vav-Cre/ERK5 $^{loxP/loxP}$  mice to Foxp3 $^{EGFP}$  reporter mice to generate ERK5 $^{-/-}$  mice with fluorescently labeled T $_{reg}$ s. ERK5 $^{-/-}$  mice present a similar percentage of CD4 $^{+}$ CD8 $^{-}$ CD25 $^{+}$ Foxp3 $^{+}$  tT $_{reg}$ s compared with ERK5 $^{+/+}$  mice (Fig. 6D), suggesting a proper tT $_{reg}$  development, despite the enrichment in the population of tT $_{reg}$  progenitors. Remarkably, ERK5 deletion results in a reduced percentage of T $_{reg}$ s in the spleen (Fig. 6E). In summary, ERK5 $^{-/-}$  mice show an augmented presence of tT $_{reg}$  progenitors and a reduced percentage of T $_{reg}$ s in the spleen, with both phenomena apparently unrelated, considering the normal development of the tT $_{reg}$  population.

## DISCUSSION

In the present study, we used different models to demonstrate that ERK5 has a dual role with antagonistic effects in the modulation of TCR/CD3 complex levels at the cell surface. On 1 hand, ERK5 knockdown or inhibition of ERK5 autophosphorylation leads to reduced amounts of the TCR/CD3 complex at the cell surface after anti-CD3 $\epsilon$  stimulation. On the other hand, we show several evidences suggesting that ERK5 promotes CD3 $\zeta$  degradation during anti-CD3 $\epsilon$  stimulation, leading to diminished TCR/CD3 levels at the cell surface. First, knockdown of ERK5 in Jurkat cells resulted in increased amounts of CD3 $\zeta$  without affecting CD3 $\epsilon$ , which led to higher cell-surface levels of TCR/CD3 (Figs. 1 and 2). Second, inhibition of MEK5-dependent phosphorylation of ERK5 in Jurkat and human T CD4 $^{+}$  cells impaired TCR/CD3 down-regulation after anti-CD3 $\epsilon$  stimulation (Fig. 3). Although ERK5 inhibitors are a proposed therapeutic approach for different cancers [24, 25], our results suggest that such treatment could produce undesired effects on T cell development. Third, DP thymocytes from ERK5 $^{-/-}$  mice showed increased CD3 $\zeta$  (Fig. 5C), probably as a consequence of altered tonic CD3 $\zeta$  ubiquitination, which is used by DP thymocytes to regulate the levels of TCR/CD3 on the cell surface [22]. Despite the small up-regulation of TCR/CD3, it could account for a shifted signaling threshold and altered selection process. Intriguingly, neither resting nor anti-CD3 $\epsilon$ -stimulated, splenic T cells from the ERK5 $^{-/-}$  mice showed altered levels of TCR/CD3 (Fig. 5B). However, we cannot discount the existence of a compensatory phenomenon or the possibility that different TCR/CD3 ligands or longer incubation times could lead to effects similar to those observed in the LAPTM5 $^{-/-}$  mice, which shows impaired TCR down-regulation in splenic T cells by promoting lysosomal degradation of CD3 $\zeta$  after anti-CD3 $\epsilon$  stimulation [26]. This point merits further study.

It was recently proposed that 2 different pathways were able to degrade CD3 $\zeta$  [27]. These included a LAPTM5-dependent pathway, which promotes degradation of intracellular CD3 $\zeta$  before assembly in the Golgi apparatus with the TCR- $\alpha\beta$ CD3 $\gamma\epsilon$ CD3 $\delta\epsilon$  complex [21], and a SLAP/c-Cbl pathway [28], which promotes degradation of recently internalized CD3 $\zeta$  from the cell surface [4, 29]. We show that ERK5-deficient DP thymocytes display a similar phenotype to LAPTM5-deficient DP thymocytes [26] but that this is less intense than in the SLAP- or

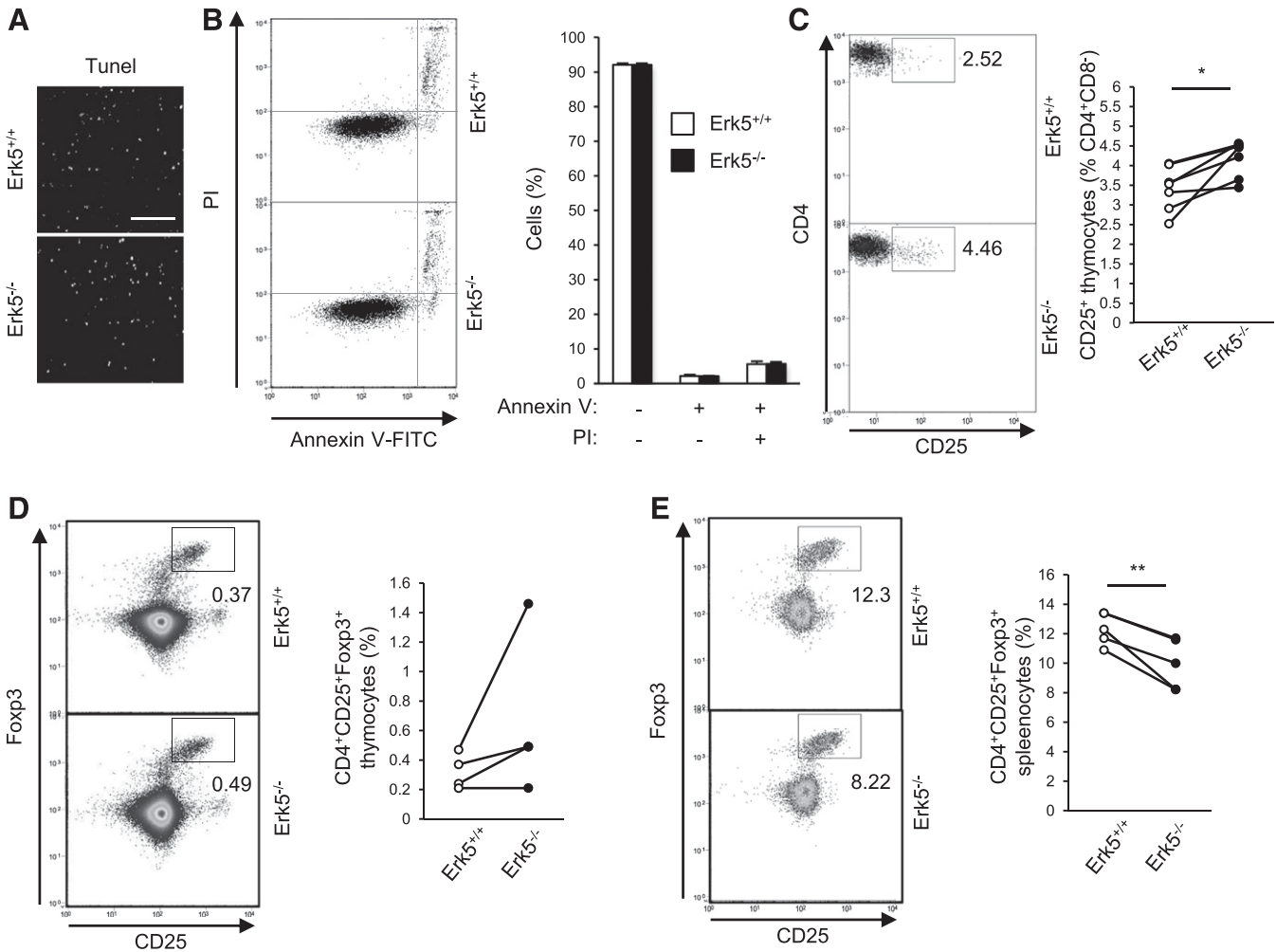


**Figure 6.** ERK5<sup>-/-</sup> mice show increased percentage of CD4<sup>+</sup>CD8<sup>-</sup>CD25<sup>+</sup> thymocytes and reduced percentage of T<sub>reg</sub> in the spleen. (A) In situ TUNEL staining on thymus sections. Representative images of 1 of the 3 pairs of ERK5<sup>+/+</sup> and ERK5<sup>-/-</sup> mice analyzed. Original scale bar, 100  $\mu$ m. Contrast and brightness have been adjusted to the entire figure to facilitate its visualization. (B) Apoptosis on thymocytes, which were stained in binding buffer with Annexin V-FITC (1:40 dilution) and propidium iodide (PI; 0.4  $\mu$ g/ml) and analyzed by flow cytometry. Representative flow cytometric profiles (left). The percentages of Annexin V-positive or propidium iodide-positive cells in ERK5<sup>+/+</sup> ( $n = 2$ ) and ERK5<sup>-/-</sup> ( $n = 2$ ) mice are shown (right). (C) Percentages of CD4<sup>+</sup>CD8<sup>-</sup>CD25<sup>+</sup> thymocytes, which were stained with anti-CD4-APC, anti-CD8-FITC, and anti-CD25-PE and analyzed by flow cytometry. Representative flow cytometric profiles of cell-surface staining/gating in CD4<sup>+</sup>CD8<sup>-</sup> population (left). The percentages of 7 pairs of ERK5<sup>+/+</sup> and ERK5<sup>-/-</sup> mice are shown (right). Differences were compared by use of paired Student's *t* test. (D and E) Flow cytometry analysis of tT<sub>reg</sub> (D) and spleen (E) from ERK5<sup>-/-</sup>-Fopx3<sup>EGFP</sup> and ERK5<sup>+/+</sup>-Fopx3<sup>EGFP</sup> mice. Cells were stained with anti-CD4-APC and anti-CD25-PE and analyzed by flow cytometry. Representative flow cytometric profiles of cell-surface staining/gating in CD4<sup>+</sup> populations (left). The percentages of ERK5<sup>+/+</sup> ( $n = 4$ ) and ERK5<sup>-/-</sup> ( $n = 4$ ) mice are shown (right). Differences were compared by use of paired Student's *t* test. \* $P < 0.05$ ; \*\* $P < 0.01$ .

c-Cbl-deficient DP thymocytes. Conversely, ERK5 inhibition in T CD4<sup>+</sup> cells showed that ERK5 was involved in the ubiquitination and degradation of recently internalized CD3 $\zeta$  (Fig. 4), suggesting that ERK5 could be involved in the regulation of both pathways. Additional studies will be needed to elucidate the relationship among ERK5, SLAP/c-Cbl, and LAPTM5 signaling pathways in the control of CD3 $\zeta$  traffic and degradation.

The development of tT<sub>reg</sub> comprises 2 stages [30, 31]: in the 1st stage, SP CD4<sup>+</sup>CD25<sup>+</sup>Fopx3<sup>+</sup> thymocytes have up-regulated cell-surface CD25, a subunit of the high-affinity IL-2R; in the 2nd stage (CD4<sup>+</sup>CD25<sup>+</sup>Fopx3<sup>+</sup>), *Fopx3* is induced. The former is TCR/CD3 dependent, and the latter is TCR/CD3 independent and IL-2 dependent [30, 31]. We propose that the up-regulation

of TCR/CD3 on DP thymocytes in ERK5<sup>-/-</sup> mice could account for the shift toward a CD4<sup>+</sup>CD25<sup>+</sup>Fopx3<sup>+</sup> phenotype. In addition, SLAP deficiency in mice increases the number of tT<sub>reg</sub>s [32], suggesting a role for the pathways that controls CD3 $\zeta$  degradation.

In conclusion, our study identifies ERK5 as a novel kinase that modulates TCR/CD3 expression in mouse and human T cells through the control of CD3 $\zeta$  degradation and TCR/CD3 recovery after anti-CD3 $\epsilon$  treatment. Further studies will be necessary to elucidate the downstream pathways activated by ERK5 that mediate CD3 $\zeta$ -chain degradation, as well as the implications of this phenomenon in T cell activation and T<sub>reg</sub> development and function.

## AUTHORSHIP

X.R.-C. conceived of, designed, and performed most of the experiments. M.A.-I. and E.E. designed and performed experiments. C.T. provided Erk5<sup>loxP/loxP</sup> mice. X.R.-C., M.A.-I., M.R., and E.E. analyzed the data. X.R.-C., M.R., and E.E. wrote the manuscript.

## ACKNOWLEDGMENTS

This work was supported by Grant FBG300412 from Fundació Bosch i Gimpera (to M.R.). X.R.-C. and M.A.-I. are supported by a predoctoral fellowship from Fundació Bosch i Gimpera (FBG300412). The authors thank the technical staff of the FACS Facility, the staff of the Animal Facility for maintaining the mice, and members of the M.R. laboratory for comments and suggestions.

## DISCLOSURES

The authors declare no competing financial interests.

## REFERENCES

- Schrum, A. G., Turka, L. A., Palmer, E. (2003) Surface T-cell antigen receptor expression and availability for long-term antigenic signaling. *Immunol. Rev.* **196**, 7–24.
- Von Essen, M., Bonefeld, C. M., Siersma, V., Rasmussen, A. B., Lauritsen, J. P. H., Nielsen, B. L., Geisler, C. (2004) Constitutive and ligand-induced TCR degradation. *J. Immunol.* **173**, 384–393.
- Liu, H., Rhodes, M., Wiest, D. L., Vignali, D. A. (2000) On the dynamics of TCR:CD3 complex cell surface expression and downmodulation. *Immunity* **13**, 665–675.
- Naramura, M., Jang, I.-K., Kole, H., Huang, F., Haines, D., Gu, H. (2002) c-Cbl and Cbl-b regulate T cell responsiveness by promoting ligand-induced TCR down-modulation. *Nat. Immunol.* **3**, 1192–1199.
- Starr, T. K., Jameson, S. C., Hogquist, K. A. (2003) Positive and negative selection of T cells. *Annu. Rev. Immunol.* **21**, 139–176.
- Kortum, R. L., Rouquette-Jazdarian, A. K., Samelson, L. E. (2013) Ras and extracellular signal-regulated kinase signaling in thymocytes and T cells. *Trends Immunol.* **34**, 259–268.
- Nithianandarajah-Jones, G. N., Wilm, B., Goldring, C. E. P., Müller, J., Cross, M. J. (2012) ERK5: structure, regulation and function. *Cell. Signal.* **24**, 2187–2196.
- Kato, Y., Kravchenko, V. V., Tapping, R. I., Han, J., Ulevitch, R. J., Lee, J. D. (1997) BMK1/ERK5 regulates serum-induced early gene expression through transcription factor MEF2C. *EMBO J.* **16**, 7054–7066.
- Regan, C. P., Li, W., Boucher, D. M., Spatz, S., Su, M. S., Kuida, K. (2002) Erk5 null mice display multiple extraembryonic vascular and embryonic cardiovascular defects. *Proc. Natl. Acad. Sci. USA* **99**, 9248–9253.
- Tatake, R. J., O'Neill, M. M., Kennedy, C. A., Wayne, A. L., Jakes, S., Wu, D., Kugler, S. Z., Jr., Kashem, M. A., Kaplita, P., Snow, R. J. (2008) Identification of pharmacological inhibitors of the MEK5/ERK5 pathway. *Biochem. Biophys. Res. Commun.* **377**, 120–125.
- Yang, Q., Deng, X., Lu, B., Cameron, M., Fearn, C., Patricelli, M. P., Yates III, J. R., Gray, N. S., Lee, J.-D. (2010) Pharmacological inhibition of BMK1 suppresses tumor growth through promyelocytic leukemia protein. *Cancer Cell* **18**, 258–267.
- Sohn, S. J., Lewis, G. M., Winoto, A. (2008) Non-redundant function of the MEK5-ERK5 pathway in thymocyte apoptosis. *EMBO J.* **27**, 1896–1906.
- Garaude, J., Kaminski, S., Cherni, S., Hipskind, R. A., Villalba, M. (2005) The role of ERK5 in T-cell signalling. *Scand. J. Immunol.* **62**, 515–520.
- Ananieva, O., Macdonald, A., Wang, X., McCoy, C. E., McIlrath, J., Tourmier, C., Arthur, J. S. C. (2008) ERK5 regulation in naïve T-cell activation and survival. *Eur. J. Immunol.* **38**, 2534–2547.
- Sohn, S. J., Li, D., Lee, L. K., Winoto, A. (2005) Transcriptional regulation of tissue-specific genes by the ERK5 mitogen-activated protein kinase. *Mol. Cell. Biol.* **25**, 8553–8566.
- Weinreich, M. A., Jameson, S. C., Hogquist, K. A. (2011) Postselection thymocyte maturation and emigration are independent of IL-7 and ERK5. *J. Immunol.* **186**, 1343–1347.
- Stadtfeld, M., Graf, T. (2005) Assessing the role of hematopoietic plasticity for endothelial and hepatocyte development by non-invasive lineage tracing. *Development* **132**, 203–213.
- Rovira-Clavé, X., Angulo-Ibáñez, M., Noguer, O., Espel, E., Reina, M. (2012) Syndecan-2 can promote clearance of T-cell receptor/CD3 from the cell surface. *Immunology* **137**, 214–225.
- Rovira-Clavé, X., Angulo-Ibáñez, M., Reina, M., Espel, E. (2014) The PDZ-binding domain of syndecan-2 inhibits LFA-1 high-affinity conformation. *Cell. Signal.* **26**, 1489–1499.
- D'Oro, U., Munitic, I., Chacko, G., Karpova, T., McNally, J., Ashwell, J. D. (2002) Regulation of constitutive TCR internalization by the ζ-chain. *J. Immunol.* **169**, 6269–6278.
- Yudushkin, I. A., Vale, R. D. (2010) Imaging T-cell receptor activation reveals accumulation of tyrosine-phosphorylated CD3ζ in the endosomal compartment. *Proc. Natl. Acad. Sci. USA* **107**, 22128–22133.
- Wang, H., Holst, J., Woo, S. R., Guy, C., Bettini, M., Wang, Y., Shafer, A., Naramura, M., Mingueau, M., Dragone, L. L., Hayes, S. M., Malissen, B., Band, H., Vignali, D. A. (2010) Tonic ubiquitylation controls T-cell receptor:CD3 complex expression during T-cell development. *EMBO J.* **29**, 1285–1298.
- Moran, A. E., Holzapfel, K. L., Xing, Y., Cunningham, N. R., Maltzman, J. S., Punt, J., Hogquist, K. A. (2011) T cell receptor signal strength in Treg and iNKT cell development demonstrated by a novel fluorescent reporter mouse. *J. Exp. Med.* **208**, 1279–1289.
- Álvarez-Fernández, S., Ortiz-Ruiz, M. J., Parrott, T., Zaknoen, S., Ocio, E. M., San Miguel, J., Burrows, F. J., Esparís-Ogando, A., Pandiella, A. (2013) Potent antimyeloma activity of a novel ERK5/CDK inhibitor. *Clin. Cancer Res.* **19**, 2677–2687.
- Shukla, A., Miller, J. M., Cason, C., Sayan, M., MacPherson, M. B., Beuschel, S. L., Hillegass, J., Vacek, P. M., Pass, H. I., Mossman, B. T. (2013) Extracellular signal-regulated kinase 5: a potential therapeutic target for malignant mesotheliomas. *Clin. Cancer Res.* **19**, 2071–2083.
- Ouchida, R., Yamasaki, S., Hikida, M., Masuda, K., Kawamura, K., Wada, A., Mochizuki, S., Tagawa, M., Sakamoto, A., Hatano, M., Tokuhisa, T., Koseki, H., Saito, T., Kurosaki, T., Wang, J.-Y. (2008) A lysosomal protein negatively regulates surface T cell antigen receptor expression by promoting CD3zeta-chain degradation. *Immunity* **29**, 33–43.
- Kawai, Y., Ouchida, R., Yamasaki, S., Dragone, L., Tsubata, T., Wang, J. Y. (2014) LAPTM5 promotes lysosomal degradation of intracellular CD3ζ but not of cell surface CD3ζ. *Immunol. Cell Biol.* **92**, 527–534.
- Myers, M. D., Sosinowski, T., Dragone, L. L., White, C., Band, H., Gu, H., Weiss, A. (2006) Src-like adaptor protein regulates TCR expression on thymocytes by linking the ubiquitin ligase c-Cbl to the TCR complex. *Nat. Immunol.* **7**, 57–66.
- Myers, M. D., Dragone, L. L., Weiss, A. (2005) Src-like adaptor protein down-regulates T cell receptor (TCR)-CD3 expression by targeting TCRzeta for degradation. *J. Cell Biol.* **170**, 285–294.
- Lio, C.-W. J., Hsieh, C.-S. (2008) A two-step process for thymic regulatory T cell development. *Immunity* **28**, 100–111.
- Burchill, M. A., Yang, J., Vang, K. B., Moon, J. J., Chu, H. H., Lio, C.-W. J., Vegoe, A. L., Hsieh, C.-S., Jenkins, M. K., Farrar, M. A. (2008) Linked T cell receptor and cytokine signaling govern the development of the regulatory T cell repertoire. *Immunity* **28**, 112–121.
- Peterson, L. K., Shaw, L. A., Joetham, A., Sakaguchi, S., Gelfand, E. W., Dragone, L. L. (2011) SLAP deficiency enhances number and function of regulatory T cells preventing chronic autoimmune arthritis in SKG mice. *J. Immunol.* **186**, 2273–2281.

## KEY WORDS:

MAPK · TCR down-regulation · ubiquitination · regulatory T cell